A MULTIVARIABLE ADAPTIVE CONTROL STRATEGY TO REGULATE THE SEPARATED FLOW BEHIND A BACKWARD-FACING STEP

M. Garwon and R. King[1]

Institute of Process and Plant Technology
Berlin University of Technology
Hardenbergstraße 36a,10623 Berlin, Germany

Abstract: Two adaptive feedback control methods, an automatically tuned PI-controller and the extremum-seeking controller are employed to control a detached flow with strictly non-linear dynamics. For the experimental validation conducted in a wind tunnel the backward-facing step flow is investigated. The experiments confirm that the presented control strategy can be used successfully to regulate this type of flow, and thus, to reduce the negative concomitant effects of the separation.

Keywords: automatic PI tuning, extremum-seeking, flow control, backward-facing step flow

1. INTRODUCTION

Flow separation accounts for important problems in various fields. Technical devices characterised by a detached flow are for instance diffusers, airfoils, or air-conditioning plants. Effects of flow separation are commonly not desired. The lift of airfoils breaks down if the flow detaches. The pressure recovery in diffusers is reduced, or noise and vibrations are produced in air-conditioning plants by flow separation. To investigate different kinds of actuation, manipulating the detached flow, simple flow configurations were considered experimentally in the seventies. See (Fiedler and Fernholz, 1990) for a detailed list of actuation methods. In the eighties the research was focused on the understanding of the physics of the separation so that this knowledge may help to design technical devices in which the concomitant effects of a separation will be minimised. In all these investigations open-loop, but not feedback control strategies were applied, to affect the detached flow. A comprehensive study of flow separation control is given in (Greenblatt and Wygnanski, 2000). Numerical studies and first experiments with successful applications of feedback control were carried out in the nineties. Sound in a diffuser (Kwong and Dowling, 1994) and drag (Lee and Kim, 1997) induced by a detached flow were reduced effectively by means of feedback control. Since then, the area of flow control is expanding at a fast rate, but is still in a premature state. The objective of the work presented here, is to regulate a detached flow using adaptive feedback control. A standard configuration characterised by a separation, namely a backward-facing step, is considered as a benchmark. Experiments are carried out in a wind tunnel to show the practicability of the proposed method.

The paper is organised as follows: in the next section, the flow configuration and some essential characteristics of this flow type and the surrogate control variable are described. In section 3, the adaptive control scheme based on the recursive estimation of an underlying process model is introduced. The results of the controlled separated flow are shown in section 4, followed by section 5, where a modification of the estimation algorithm is motivated and explained. The paper ends with a conclusion.

2. FLOW CONFIGURATION AND SOME FUNDAMENTAL CHARACTERISTICS

[1] Corresponding author, email: rudibert.king@tu-berlin.de,

The flow over a backward-facing step is a simple flow configuration with a fixed separation, see **Fig. 1**. This kind of flow can be viewed, for example, as a prototype of a flow inside a burner. In a highly simplified picture the flow looks as follows. Because of its inertia, the oncoming flow, with a free-stream velocity U_∞, is not able to follow the sudden expansion at the step. Therefore, the flow detaches at this position. The main flow moves on above a recirculation bubble and reattaches at the bottom wall at a location x_R downstream of the step. The flow in the recirculation bubble is a secondary flow. In a first very crude approximation, this flow can be imagined as a rotating vortex. Near the main flow, this secondary flow moves in the same direction, and reverse close to the bottom wall. The energy required for the rotation is extracted from the main flow itself.

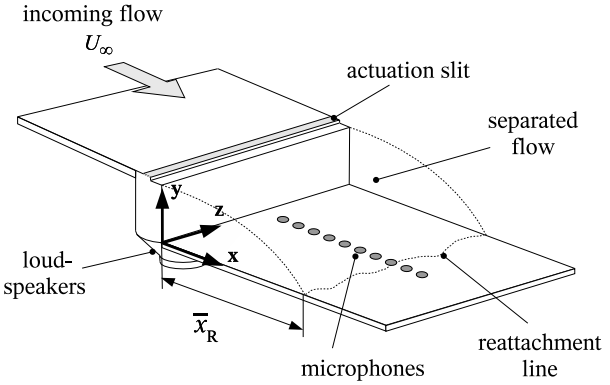

Fig. 1. Flow configuration: The backward-facing step with loudspeakers used for actuation.

Between the main and the secondary flow a shear flow develops, which is characterised by an instability process with the natural Kelvin-Helmholtz instability frequency $f(t)$. A widely accepted method to control separated flows, is to introduce disturbances at the separation location, i.e. at the edge of the step (Greenblatt and Wygnanski, 2000). This is done most efficiently by an actuation with the natural instability frequency. It is generated by loudspeakers supplied with a periodic voltage signal $u(t)$,

$$u(t) = u_0(t)\cdot\sin(2\pi\ f(t)\cdot t). \tag{1}$$

The time-dependent amplitude $u_0(t)$ and the forcing frequency $f(t)$ are the input variables of the plant to be controlled. The plant output, which characterises the length of the flow separation, is the dimensionless reattachment length x_R/H, with H being the step height. The reattachment length is defined by a zero-mean wall-shear stress τ_w

$$\tau_w = \eta\cdot\left.\frac{\partial\bar{u}}{\partial y}\right|_{y=0} \tag{2}$$

with η being the dynamic viscosity of the fluid. y is the co-ordinate vertical to the bottom wall and $\bar{u}$ denotes the component of the time-averaged velocity in the x-direction, i.e. the direction of the mean flow. The spanwise and time-averaged wall-shear stress in the wake of the step, obtained from a numerical solution of the governing equations, the Navier-Stokes-Equations, is given in **Fig. 2a**. The Reynolds number, regarded here as the dimensionless free-stream velocity (3), is Re_H=4000.

$$Re_H = \frac{U_\infty\cdot H}{\nu} \tag{3}$$

Due to the reverse near-wall flow the wall-shear stress in the wake becomes negative over a wide range (x/H=2...6.4). The wall-shear stress vanishes at the location x/H=6.4, hence, the main flow reattaches at this position (**Fig. 2a**).

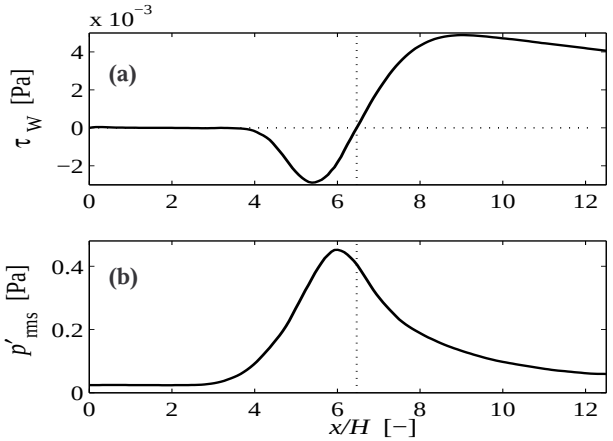

Fig. 2. Wall-shear stress (a) and wall pressure fluctuations (root-mean-square value) in the wake of the step. The x-direction is normalised by the step height H.

A surrogate variable for the reattachment length

Several techniques to measure the wall-shear stress exist. However, these techniques are very expensive, not practical for our purpose, and a large time-averaging is required for an accurate measurement of the wall-shear stress. An appropriate choice, determining the reattachment length indirectly, is to measure the wall-pressure fluctuations in the wake of the step by microphones. Several authors have confirmed that the root-mean-square (rms) value

$$p'_{rms} = \sqrt{\overline{p'^2}} \tag{4}$$

of wall-pressure fluctuations p' rises to a maximum in the reattachment region (Mabey, 1972), see **Fig. 2b**.

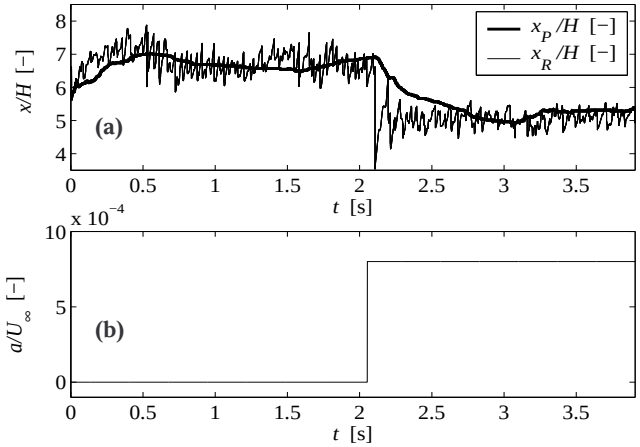

Fig. 3. Step response of the instantaneous reattachment length x_R/H and the surrogate length x_P/H based on the wall-pressure fluctuations behind a backward-facing step. Large-Eddy-Simulation (LES) at Re_H=4000.

The location of maximal pressure fluctuations varies slightly between $0.85...0.95 \cdot x_R$, and this relation is valid for a wide range of Reynolds numbers, forcing amplitudes and frequencies. To determine the root-mean-square value, a time-averaging is needed. Experiments have shown that time-averaging of about one second is necessary to obtain this relation.

Fig. 3a illustrates the step response of the instantaneous, i.e. spanwise, but not time averaged reattachment length x_R/H and the dimensionless surrogate variable x_P/H, based on the rms value of the wall-pressure fluctuations. Switching the actuation on, the flow reacts after a short dead-time of about T_0=0.08s with a strong sudden reduction of the instantaneous reattachment length (**Fig. 3a**, thin line). Subsequently, the plant output converges to its new state with a saw-tooth type motion caused by vortex processes in the shear-layer. See (Becker *et al.*, 2003) for more details about the vortex processes. In contrast, due to the averaging time, a slower dynamic can be observed in the time series of the surrogate variable x_P (**Fig. 3a**, thick line). Important for the closed-loop control is that the difference between the steady state values of both variables can be neglected.

Recent investigations of a backward-facing step flow (Wengle, et al., 2001) confirm that the reattachment length depends in a non-linear fashion on the two input variables which are the amplitude and the frequency of the sinusoidal signal $u(t)$. At first, the process is characterised by an output saturation (**Fig. 4a**). Additionally, more than one locally optimal frequency exists for a fixed Reynolds number and a fixed amplitude (**Fig. 4b**). Experiments also confirm that a higher Reynolds number shifts the optimal forcing frequency to higher values, shown here for Re_H=4000 and Re_H=10000, respectively.

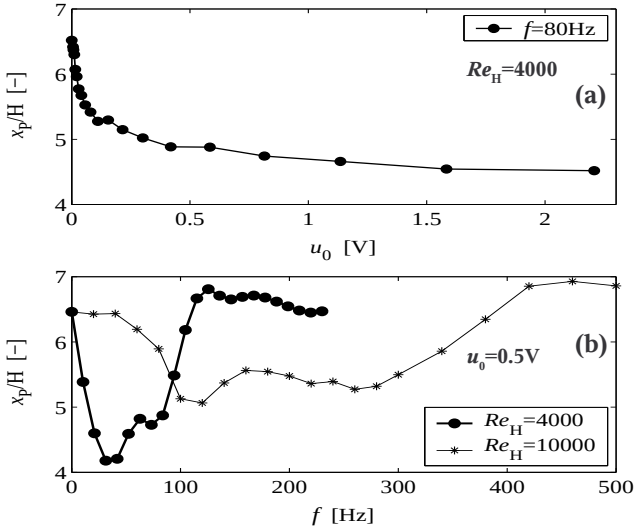

Fig. 4. The surrogate variable as a function of the forcing amplitude (a) and the forcing frequency of the control signal, see eq. (1), for different Reynolds numbers (b).

It should be mentioned that the flow reacts less sensitive when the Reynolds number is increased. That means, to achieve a desired reduction of the reattachment length higher amplitudes are necessary at higher Reynolds numbers. The reader is referred to (Wengle, *et al.*, 2001) for more details of these complex flow properties.

Finally, in (Becker, *et al.*, 2002) it is shown that the input/output behaviour between $u_0(t)$ and $x_P(t)$ can be approximated by a family of linear first or second order black-box models with dead-time.

3. ADAPTIVE CONTROL ALGORITHMS

Flows are characterised by a highly non-linear behaviour of infinite dimension. Rigorous mathematical modelling leads to the well-known Navier-Stokes-Equations (NSE), i.e. a set of non-linear PDEs. Attempts to build up controllers based on the NSE (Bewley, 1998) lead to control laws, which are far from being applicable in a real-time environment in the near future. Therefore, other means of controller synthesis are needed. Examples are controllers derived from low-dimensional approximations of NSE (Pastoor, *et al.*, 2003), or controllers based on simple, experimentally obtained models (Becker, *et al.*, 2003; King *et al.*, 2004). Adaptive concepts are also promising candidates for the latter category.

Scheme of the closed-loop

The scheme of the proposed control strategy is illustrated in **Fig. 5**.

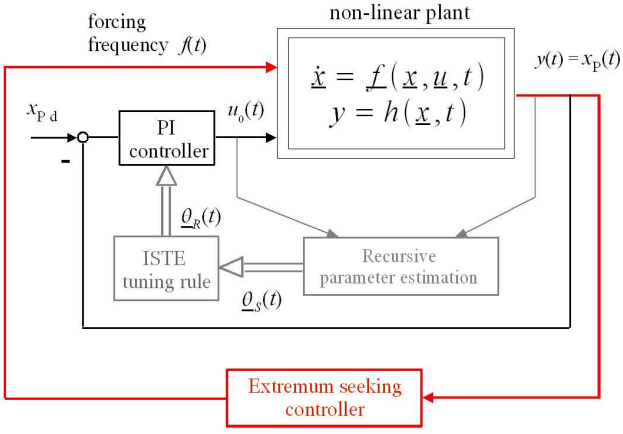

Fig. 5. Scheme of the proposed closed-loop.

It is a combination of an automatically tuned PI-controller calculating the forcing amplitude $u_0(t)$, and the extremum-seeking controller (Krstic, 2000) determining the optimal forcing frequency $f(t)$. A PI-controller is chosen because the input-output response of the step flow can be approximated by simple black-box models of first or second order (Becker, *et al.*, 2003). The controller parameters $\underline{\theta}_R$ are calculated by the ISTE tuning rules (Zhuang and Atherton, 1993), based on a continuous estimation of a model with a set of parameters $\underline{\theta}_S$ describing the actual process dynamics. This controller is placed in the inner loop, a classical control-loop with a comparison between the actual plant output x_P and its desired value x_{Pd}.

The aims of the inner loop are tracking of the reference x_{Pd} and rejecting disturbances. An extremum-seeking controller is employed and placed in the outer loop to achieve these aims by a minimal consumption of control energy.
The extremum-seeking controller varies the forcing frequency $f(t)$ harmonically, i.e.

$$f(t) = f_0 + \Delta f \sin(\omega \cdot t), \tag{5}$$

such that a gradient information towards an optimal frequency is obtained. For more details see (Krstic, 2000). To avoid a strong interference between these controllers in this MISO-setting, the angular frequency of the harmonic perturbation ω lies in a range where the sensitivity of the inner loop is equal to one. Hence, the oscillations of the surrogate variable caused by this harmonic perturbation can not be suppressed by the PI-controller.

Recursive estimation of the surrogate variable

To maintain a high performance of the closed-loop regulating a non-linear process, a continuous adaptation of the controller parameters is required (Isermann *et al.*, 1992). As mentioned above, simple low order models with a dead-time can be used to approximate the process behaviour. Therefore, an ARMAX model (6) with the orders *na*=1, *nb*=1, *nc*=1, and a dead-time of T_0=0.1s, i.e. a one sample delay *nk*=2, is chosen, see eq. (7). Hence, only three parameters must be estimated.

$$A(z^{-1})\,y(t) = B(z^{-1})\cdot z^{-nk}\,u(t) + C(z^{-1})\epsilon(t) \tag{6}$$

$$\begin{aligned} A(z^{-1}) &= 1 + a_1 z^{-1} + a_2 z^{-2} + \ldots + a_{na} z^{-na} \\ B(z^{-1}) &= b_1 + b_2 z^{-1} + \ldots + b_{nb} z^{-nb+1} \\ C(z^{-1}) &= 1 + c_1 z^{-1} + c_2 z^{-2} + \ldots + c_{nc} z^{-nc} \end{aligned} \tag{7}$$

Results of the used recursive extended least-square approach (RELS) based on an ARMAX model with a forgetting factor λ=0.95 are depicted in **Fig. 6**.

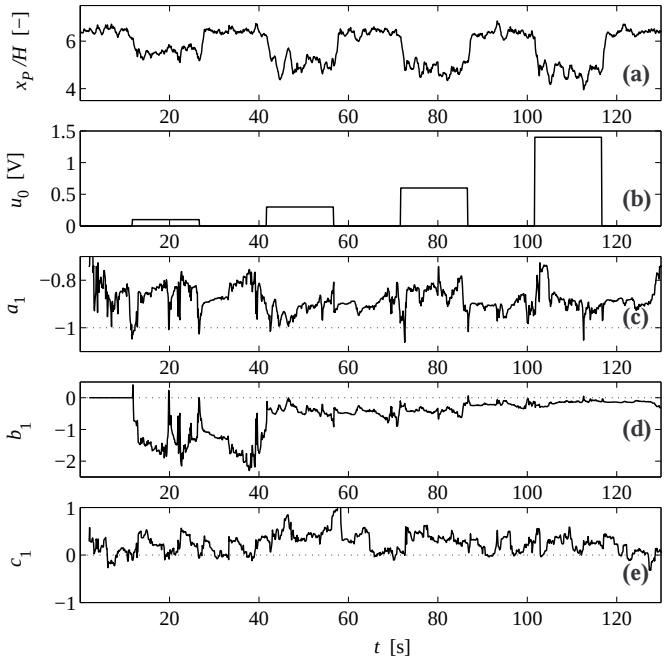

Fig. 6. Recursively estimated parameters of a first order ARMAX model at a Reynolds number Re_H=4000 (wind tunnel experiment) with *f*=80Hz.

The time series of the surrogate variable x_P/H and the plant input u_0 are plotted in the upper part, see (a) and (b). The sampling time chosen is T_S=0.1s. Some important features can be seen in the time series of the estimated parameters. Parameter b_1 in **Fig. 6d** reflects the plant feature of an output saturation, i.e. a stronger actuation leads to a smaller amount of the parameter b_1 whilst the parameter a_1 oscillates around its mean value $\bar{a}_1$=-0.88. Hence, the static gain of the process model decreases with an increasing strength of the actuation. In contrast, the parameter c_1 even changes its sign and oscillates with a large amplitude. Hence, the disturbances model does not describe the influence of disturbances $\epsilon(t)$ well. Other orders for the dynamic model, especially for the disturbance part, were chosen, but an improvement could not be achieved (results not shown).

Because of the strong oscillations of all estimated parameters, with the parameter b_1 of the numerator being positiv sometimes, and the parameter a_1 of the denominator less than -1, low-pass filtered values of the parameters must be used in the tuning rules to calculate the controller parameters. An additional phase shift, resulting in a slower dynamics of the estimation algorithm, is obtained, consequently.

4. RESULTS OF THE CLOSED-LOOP

First experiments demonstrated that a direct application of the ISTE tuning rules yields an unstable closed-loop behaviour. This is a result of the dynamics of the estimation algorithm including the additional low-pass filtering of the estimated parameters, see section 3. Therefore, to get a more conservative tuning of the PI-controller, the plant gain used in the tuning rules was chosen three times higher than the estimated one and the dead-time used in the rules was increased to T_0=0.2s.

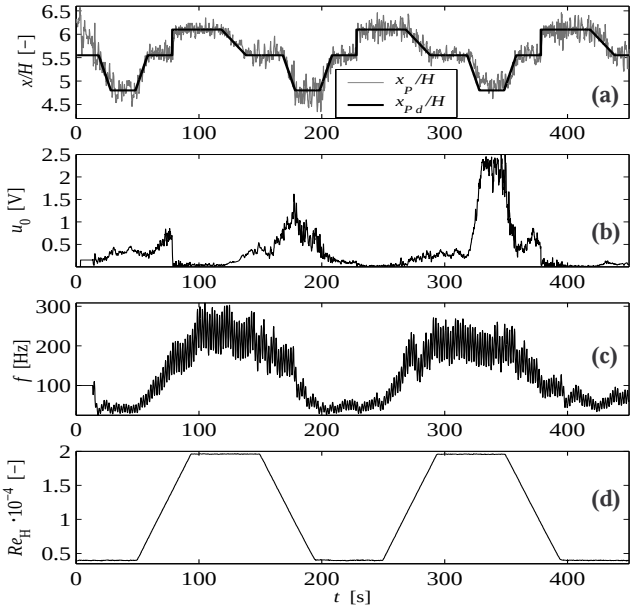

Fig. 7. Closed-loop control of the reattachment length behind a backward-facing step at variable Reynolds numbers (wind tunnel experiment).

The results of the conservatively tuned closed-loop are depicted in **Fig. 7**. Independently of the changing Reynolds number the closed-loop tracks the reference (**Fig. 7a**). The overlaying disturbances, seen especially at low Reynolds numbers, are the result of the extremum-seeking controller.

The oscillations, as mentioned above, can not be rejected by the PI-controller. To improve the performance of the extremum-seeking controller, an increased seeking radius, enhancing the sensitivity of the seeking algorithm, is implemented for higher optimal frequencies, i.e. for higher Reynolds numbers. This is a consequence of the plant characteristics that the slope of the static map diminishes when the Reynolds number is increased, see **Fig. 4b**.

Nevertheless, the limited performance of the inner loop can be seen when the Reynolds number is large (t>320s). Although the extremum-seeking controller finds the optimal forcing frequency again, the PI-controller does not increase the amplitude fast enough to track the reference. This is a result of the dynamics of the recursive estimation algorithm. To avoid such transients a faster estimation of the process dynamics resulting in a faster adaptation of the controller must be aspired.

5. MODIFICATION OF THE RECURSIVE ESTIMATION

In this section a modification of the recursive estimation approach is presented. This modification bases on a splitting up of the whole process dynamics into sensor dynamics and flow dynamics. Approximating the sensor dynamics by a first order transfer function and assuming that the real flow dynamics is faster than the sensor dynamics, a faster estimation algorithm and, consequently, a faster adaptation of the controller parameters can be achieved.

The idea for the modification

Assume that the time constants of the flow dynamics are very small and the instantaneous wall-pressure distribution has the same shape as the corresponding rms distributions. In this case, switching the actuation on, e.g. u_0=0V→0.6V, the flow changes its state very fast accompanied by a new wall-pressure distribution (**Fig. 8a**). Taking the first wall-pressure distribution (for u_0=0V) as the input of the rms sensor, see section 2, with an averaging-time of one second the sensor output is then x_P=6.3H (**Fig. 8b**, t<2s). Only the sensor algorithm is considered here, without the flow dynamics. At time t=2s the second distribution (for u_0=0.6V) is used as the sensor input. Passing it through the sensor, the sensor output reduces about 1.5 step heights after a transient caused by the receding horizon averaging process, see the thick line in **Fig. 8b**. The transient can be approximated by a first order transfer function without a dead-time (**Fig. 8b**, thin line). The time constant of the transfer function is estimated to τ_P=0.45s. The real flow process possesses its own additional dynamics. Therefore, it is assumed that the whole dynamics consists of the fixed sensor dynamics and the flow dynamics are in series.

The whole dynamics can be approximated by a first order plus dead-time transfer function (8) with an (invariant) time constant of τ_P=0.45s.

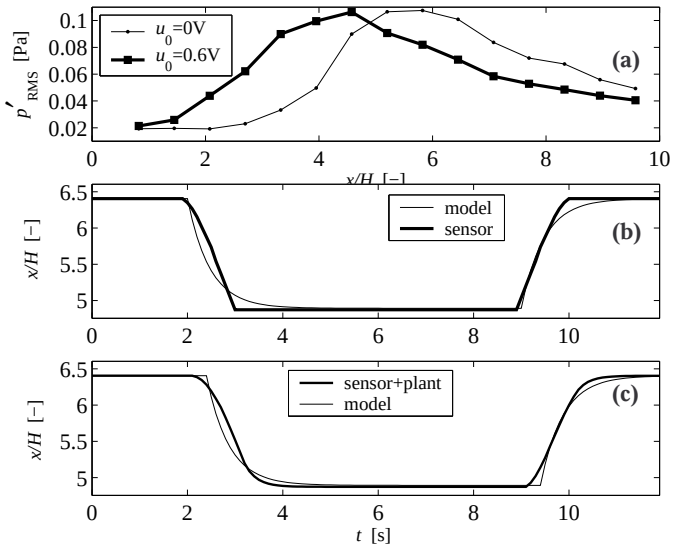

Fig. 8. RMS value distribution for a natural and a manipulated flow (a) and the response of an estimated model describing the non-linear sensor dynamics (b), (c).

The dead-time (9) is the sum of the overall flow time constant and the dead-time of the flow (to be estimated), see **Fig. 8c**.

$$G(s) = \frac{K_P}{\tau_P \cdot s + 1} \mathrm{e}^{T_0 s} \tag{8}$$

$$T_0 = \tau_{process} + T_{0\,process} \tag{9}$$

In the first part of the transients this approximation is not perfect. The accuracy of the approximation decreases when the time constants of the flow process increase. To estimate the dead-time, the order of the numerator polynomial $B(z^{-1})$ of the transfer function (7) is set to nb=4, i.e. a maximal dead-time of T_0=0.3s is assumed. The time constant is fixed to τ_P=0.45s or a_1=-0.8, respectively, and nk is set to one.

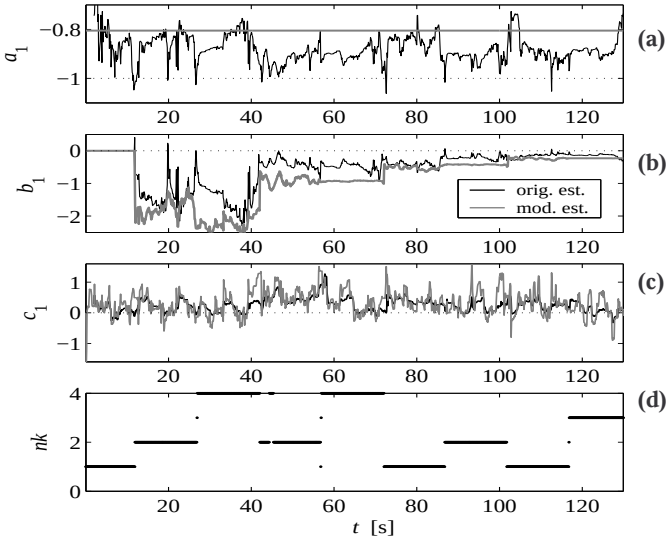

Fig. 9. Estimated parameters of an ARMAX model at a Reynolds number Re_H=4000 exploiting an approximation of the non-linear sensor dynamics.

The model parameters estimated by the modified algorithm (thick line) compared with the original estimated model

parameters (thin line, see also **Fig. 6**) and the estimated dead-time are depicted in **Fig. 9**.

The faster dynamics of the estimation algorithm is achieved because a smaller forgetting factor λ=0.85 could be used. It must be noted that the smaller forgetting factor does not cause stronger oscillations in the time series of the estimated parameter b_1. In contrast, the oscillations of the parameter c_1 are increased slightly. The estimated dead-time (**Fig. 9d**) varies between the time spans of actuation, but no relation between the dead-time.

Using this modified estimation algorithm, the ISTE tuning rules can now be applied directly. The performance of the closed-loop is shown in **Fig. 10**. The closed-loop tracks also the time-dependent reference variable during an experiment with faster transients, compare with **Fig. 7**.

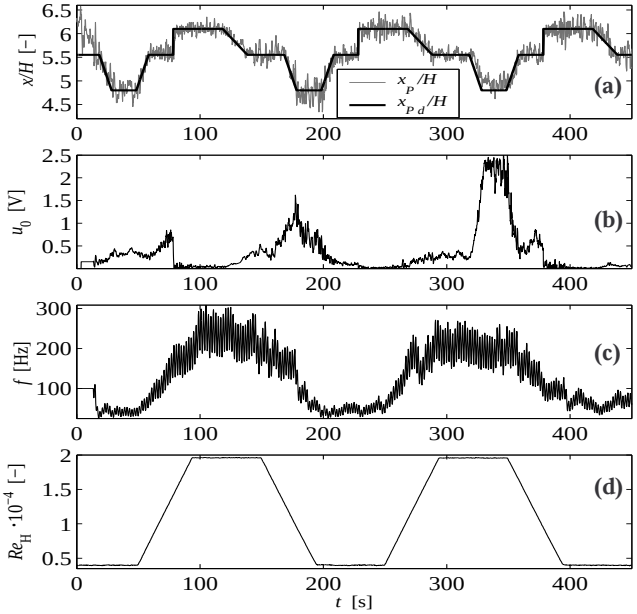

Fig. 10. Closed-loop control of the surrogate variable describing the reattachment length for variable Reynolds numbers.

An important feature of this experiment can be seen in the first part, where the reference signal is decreased. The extremum-seeking controller can not extract the right information about the gradient from the time series of the surrogate variable and the forcing frequency is hereupon increased. Consequently, higher amplitudes are calculated by the PI-controller. After that, the reference is kept constant and the extremum-seeking controller reduces the frequency followed by a reduction of the amplitude. This behaviour demonstrates that control energy can be minimised when the optimal frequency is used for actuation.

6. CONCLUSION

An automatic PI-controller and the extremum-seeking controller are used to regulate the reattachment length of a simple flow configuration. The extremum-seeking controller is necessary to find the optimal forcing frequency, which depends on the Reynolds number. So, for the reduction of the reattachment length the control energy consumed is minimised. Experiments carried out in a wind tunnel show that at variable Reynolds numbers the closed-loop tracks the reference signal, but a more conservatively tuned PI-controller must be used to avoid an unstable closed-loop. Due to a modification in the recursive estimation algorithm the dynamics of the algorithm can be increased, and a faster adaptation of the PI-controller is possible. Consequently, the performance of the closed-loop can also be improved.

REFERENCES

Becker, R., Garwon, M., and King, R. (2003). Development of model-based sensors and their use for closed-loop control of separated flows. *In Proc. of the European Control Conference ECC* 2003, Cambridge

Bewley, T. (1998). Optimal and robust control and estimation of linear paths to transition. *J. Fluid Mech.*, Vol. 365, pp. 305-349

Fiedler, H. & Fernholz, H.H. (1990). On the management and control of turbulent shear flows. *Prog. Aerospace Sci.,* Vol. 72, pp. 305-387

Greenblatt, D. & Wygnanski, I. (2000). The control of flow separation by periodic excitation. *Progress in Aerospace Science*, Vol. 36, pp. 487-545

Isermann, R., Lachmann, K.-H. & Matko, D. (1992). Adaptive control systems. *Prentice Hall International*

King, R., Becker, R., Garwon, M. & Henning, L. (2004). Robust and adaptive closed-loop control of separated shear flows. AIAA-Paper 2004-2519, *2nd AIAA Flow Control Conference*, Portland, Oregon, U.S.A., 28.6.-1.7.2004

Krstic, M. (2000). Stability of extremum seeking feedback for general non-linear dynamics systems. *Automatica*, Vol. 36, pp. 595-601

Kwong, A. & Dowling, A. (1994). Active boundary-layer control in diffusers. *AIAA Journal*, Vol. 32, No. 12

Lee, C. & Kim, J. (1997). Application of neural networks to turbulence control for drag reduction. *Phys. Fluids*, Vol. 9, (6), pp. 1740-1747

Mabey, D. (1972). Analysis and correlation of data on pressure fluctuations in separated flows. *J. Aircraft*, Vol. 9, No. 9, pp. 642-645

Wengle, H., Huppertz, A., Bärwolff, G. & Janke, G. (2001). The manipulated transitional backward-facing step flow: an experimental and direct numerical simulation investigation. *Eur. J. Mech., B/Fluids*, pp. 25-46

Zhuang, M. & Atherton, D.P. (1993). Automatic tuning of optimum PID controllers. *IEE Proc. Control theory and Appl.*, Vol. 140, No. 3